Received 25 May 2014; revised 15 June 2014 and 28 June 2014; accepted 30 June 2014. Date of publication 20 July 2014; date of current version 23 October 2014. The review of this paper was arranged by Editor A.G. Unil Perera.

Digital Object Identifier 10.1109/JEDS.2014.2341602

Optically Powered Energy Source in a Standard CMOS Process for Integration in Smart Dust Applications

JING JING LIU[1,2], GRAHAME FAULKNER[2], BHASKAR CHOUBEY[2] (Member, IEEE), JIA LIU[3], RI QING CHEN[1], DOMINIC C. O'BRIEN[2] (Member, IEEE), AND STEVE COLLINS[2] (Member, IEEE)

[1] Fujian Agriculture and Forestry University, Fuzhou 350002, China
[2] Department of Engineering Science, University of Oxford, Oxford OX1 3PJ, U.K.
[3] National Supercomputing Center, Shenzhen 518055, China

CORRESPONDING AUTHOR: S. COLLINS (steve.collins@eng.ox.ac.uk)

This work was supported by the U.K. Engineering and Physical Sciences Research Council (EPSRC) under Grant EP/D501008/1.

ABSTRACT In order to miniaturize nano-power sensor nodes or smart dust, an optically powered energy source is developed to replace traditional batteries or solar cells. This energy source consists of two photodiodes, which are P-well/DN-well and N-well/P-sub. The two photodiodes with an area of 1.5mm^2 were fabricated using the UMC 0.25μm CMOS process and tested using an 830nm laser. Measurement results show that the energy source is able to generate a voltage from 0.5V to 0.8V with a 3.5% conversion efficiency. The proposed energy source was made using a standard CMOS process and therefore can to be integrated with the smart dust circuit on a single chip.

INDEX TERMS Optically powered, source on chip, photodiodes, sensor nodes, smart dusts.

I. INTRODUCTION

The trend in the development of sensor nodes for wireless sensor networks is towards ultra-low power design, size reduction, and the ability of scavenging power [1]. As a result some sensors and communication circuits have been realized consuming nano-watts [2]–[4]. When a node integrates self-contained sensing and communication system into a cubic-millimetre mote, it is called "Smart Dust" [5]–[8]. Smart dust normally obtains energy from batteries or solar cells, which occupy a significant volume. To reduce the size of smart dust and scavenge power, the energy source can be implemented using photodiodes integrated onto the same CMOS chip as the smart dust circuits and supply the power to support the circuit's operation. Photodiodes in the standard CMOS process have various applications. Image sensors are usually made from shallow p-n junctions, which can realize a linear response [9]–[11] or a logarithmic response [12]–[14]. The optical short-distance interconnects, such as board-to-board and chip-to-chip communications, use avalanche photodiodes for high speed data transmission, which are implemented by deep p-n junctions [15], [16]. Two previous papers have described photodiodes used to create an on-chip power source [17], [18]. One of these power sources consisted of two stages. The first stage includes a few P+/N-well photodiodes connected in parallel and then they are series connected to one P+/N-well photodiode in the second stage [17]. This consumes a large chip-area and a low energy conversion efficiency of 3% is obtained. In [18], simulation results show that a two-diode voltage can be achieved by series connections of three desired p-n junctions located along a vertical line. However, the total available current of the source is small for long wavelength light illumination because it is limited by the shallow junction quantum efficiency. This paper presents an optically powered energy source in a standard CMOS process that is specifically designed to generate power from long wavelength light and is organized as follows. Section II discusses the design of the energy source. Measurement results are presented in Section III and Section IV gives the conclusions of the paper.

II. CONFIGURATION OF ENERGY SOURCE

Optical wireless communications often use invisible near infrared wavelengths and an 830nm laser was therefore selected as the wavelength for communication to a smart dust node [7]. In addition to receiving the optical signal the smart dust has been designed to generate power from the laser illumination. When a photodiode is under illumination, the voltage difference across the photodiode terminals is given by equation (1).

$$V_{photodiode} = V_T \ln\left(\frac{I_{ph} - I_L}{I_T} + 1\right) \tag{1}$$

where I_T is the reverse saturation current of the diode, V_T is thermal voltage which is approximately 25.9mV at 300K, I_{ph} is the generated photocurrent and I_L is the load current. The photocurrent for a particular optical power is then a function of quantum efficiency of the photodiode.

$$QE(\lambda) = \frac{N_{electrons}}{N_{photons}} = \frac{hcI_{ph}}{\lambda q P_{opt}} \tag{2}$$

where h is the Plank's constant, c is the speed of light, λ is the wavelength of the beam, P_{opt} is the optical power received by the power photodiode and q is the electron charge. The absorption of light, and hence the quantum efficiency of a photodiode, then depends on the photon absorption coefficient of silicon and the thickness of the material. The number of absorbed photons $F_{abs}(\lambda)$ is given by

$$F_{abs}(\lambda) = F_0(\lambda)(1 - R(\lambda))\left(1 - e^{-\alpha(\lambda)x}\right) \tag{3}$$

where $F_0(\lambda)$ is the number of photons incident on the surface, $R(\lambda)$ is the fraction of photons reflected from the surface and (1- $R(\lambda)$) is the fraction of photons entering the photodiode, $\alpha(\lambda)$ is the photon absorption coefficient, x is the depth into the photodiode. The absorption coefficient is large for short wavelength and small for long wavelength [19]. This means that short wavelength light is absorbed near the silicon surface and the longer wavelength light is absorbed deeper in the material. Therefore, for the 830nm light, deep junction diodes are expected to generate larger photocurrents than shallow junctions.

A P-N junction photodiode under illumination could generate a voltage of approximately 0.3V - 0.45V and this voltage is too low to power the smart dust system [7]. Therefore, two P-N junction photodiodes should be connected in series in order to achieve a useful voltage. This needs a triple-well CMOS process and the UMC 0.25μm CMOS process has been chosen for the design. There are six different P-N junctions available in this process; these are the N+/P-sub, P+/N-well, P+/DN-well (DN-well is deep N-well, which sits in the P-substrate and encloses a P-well.), N-well/P-sub, DN-well/P-sub and P-well/DN-well junctions. The first three junctions in this list are shallow junctions and the last three are deeper junctions. All the combinations including N+/P-sub, P+/DN-well or P+/N-well were rejected, because the shallow junctions have lower quantum efficiencies at 830nm wavelength. A cross section of the connection of two P-well/DN-well is shown in Fig. 1(a). The P side of the photodiode has a higher potential than the N side under illumination. Therefore the DN-well of one diode, shown on the left hand-side of Fig. 1(a), has to be connected to the substrate so that the P-well in this DN-well is one diode voltage above the substrate. This P-well is then connected to the DN-well of the other, right-hand diode, so that the P-well in the right diode can be two diode voltages above the substrate. Alternatively, both of N-well/P-sub and DN-well/P-sub diodes can be used in combination with P-well/DN-well. For example, the N-well on the left of Fig. 1(b) can be one diode voltage below the substrate. The DN-well on the right is connected to the substrate so that the P-well in this DN-well can generate a voltage that is one diode voltage above the substrate. Again a voltage difference of two diode voltages can be achieved.

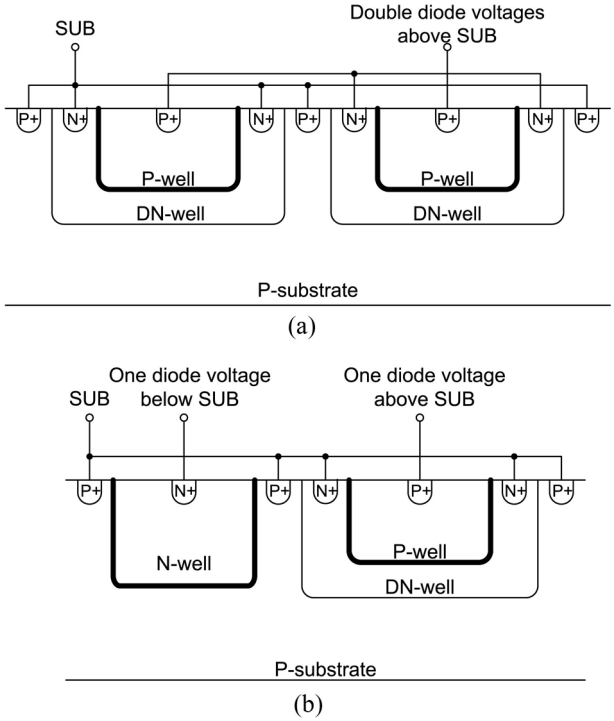

FIGURE 1. (a) 2 P-well/DN-wells. (b) N-well/P-sub and P-well/DN-well. All the bold lines in the figure represent the active junctions we use.

III. MEASUREMENT RESULTS AND DISCUSSION

A. MEASUREMENT SETUP

Different combinations of 0.75 mm^2 photodiodes were fabricated using the UMC 0.25μm CMOS process as shown in Fig. 2. The response of these photodiodes was then tested using a Newport 5005 laser driver to drive a 830nm laser diode. A metal shield with a 2.5mm diameter aperture in its centre was placed in front of the laser diode, to create a point light source. Two lenses were then used to collimate the laser beam and focus the light. The focused beam is directed to the chip by a beam splitter. The photodiode terminal voltage was measured using an Agilent 4155B when the current drawn from the diode was varied.

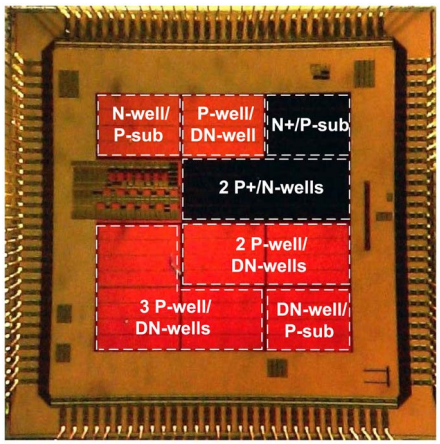

FIGURE 2. **First chip with different photodiodes fabricated using UMC 0.25μm CMOS process and each photodiode is 0.75 mm^2.**

B. SINGLE PHOTODIODES

The load line of single P-well/DN-well was measured and the quantum efficiency was found to be 7.45%. This is lower than expected and the possible reason is that the absorption depth of 830nm light is deeper than the P-well/DN-well junction. Therefore the DN-well/P-sub junction below the P-well/DN-well absorbs most of the photon-generated electrons. The load lines of N-well/P-sub, DN-well/P-sub and N+/P-sub were measured and the quantum efficiencies of them was found to be 64.64%, 70.46% and 1.68% respectively. As expected, the shallow junction N+/P-sub has the smallest quantum efficiency and is therefore a worse power source.

C. CASCADED P-WELL/DN-WELL

In order to attempt to obtain higher voltages, two P-well/DN-well or three P-well/DN-well photodiodes were connected in series. However, measurement results show that the cascaded photodiode terminal voltage is approximately 0V. A possible explanation for this failure [16] is illustrated in the Fig. 3. For the purpose of understanding, holes are used to show the movement of carriers in the photodiodes. Since the DN-well/P-sub junction absorbs more photons, only a small number of photon-generated holes move out of the left diode to the Node 1 and flow into the DN-well of the diode on the right. Most of the photon-generated carriers in the right diode are in the depletion region of DN-well/P-sub and these outnumber the holes from the left diode entering at Node 1. These holes are swept to the P-substrate by the internal field of this depletion region. Hence, the holes from the left diode are neutralized in the DN-well of the right diode.

D. ENERGY SOURCE

The P-well/DN-well and N-well/P-sub were selected to be the energy source. The measurement results show the DN-well/P-sub has a higher quantum efficiency than N-well/P-sub. However, if it is used to form the energy

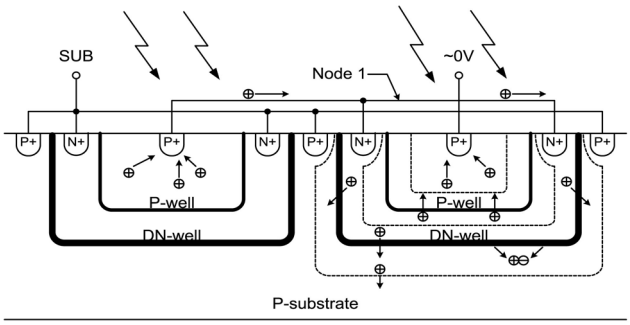

FIGURE 3. **Illustration of the failure of two P-well/DN-well photodiodes in series. Dashed line represents depletion region.**

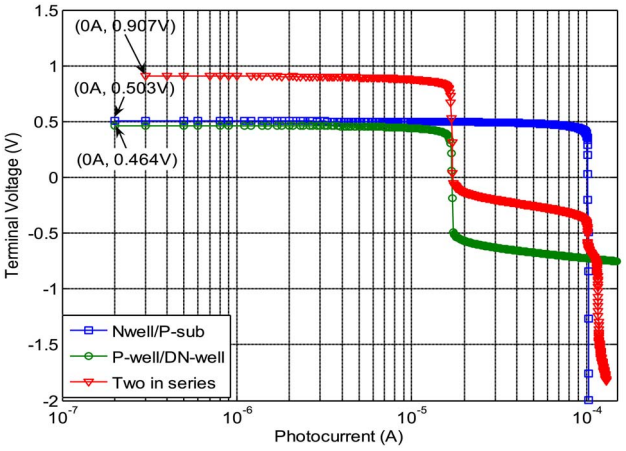

FIGURE 4. **Load lines of N-well/P-sub, P-well/DN-well and two in series.**

source with an P-well/DN-well photodiode, the two DN-wells may short. When these two photodiodes are connected in series, the terminal voltage of the two photodiodes in series is slightly smaller than the sum of the individual voltage of the two photodiodes, as shown in Fig. 4. This can be explained from the energy band diagrams in Fig. 5. When an open-circuit p-n junction is under illumination, photo-generated minority carriers flow across the depletion region and the electrochemical potential of electrons is higher in the n-type region than in the p-type region by an amount of qV_{oc}, as shown in Fig. 5(a). When the proposed energy source in Fig. 1(b) is under illumination, the P-sub and DN-well are short circuited and this means they have the same Fermi level, as shown in Fig. 5(b). The two photodiodes of the energy source are placed next to each other on the chip. This means that the photo-generated minority carriers in the P-sub and DN-well can diffuse in both directions and some photo-generated electrons in the P-sub recombine with the photo-generated holes in the DN-well. Therefore a slightly smaller open circuited voltage is achieved.

It can be seen that the maximum photocurrent to power the smart dust is limited by the P-well/DN-well photodiode due to its smaller quantum efficiency. Therefore the two photodiodes were resized with 0.2mm^2 N-well/P-sub and 1.3mm^2 P-well/DN-well. Another chip has been fabricated and its picture is shown in Fig. 6.

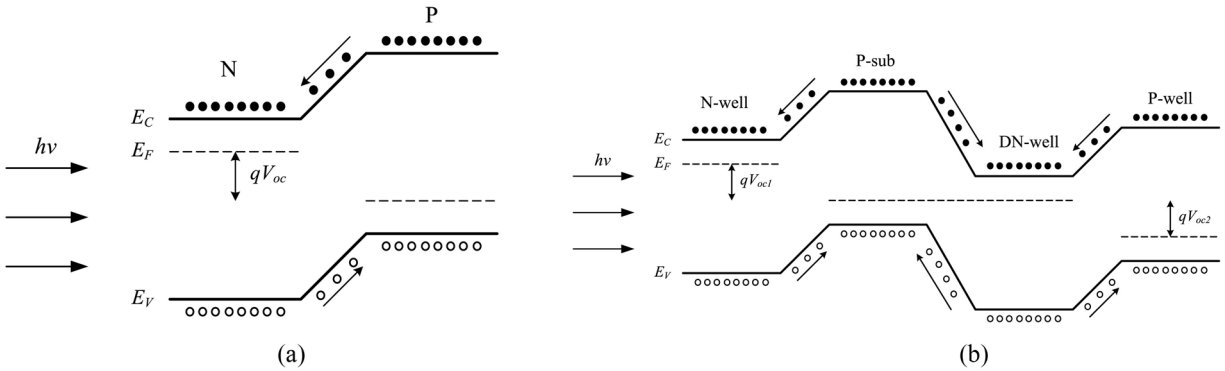

FIGURE 5. **Energy band diagrams of open-circuit photodiodes under illumination. (a) Single p-n junction. (b) Proposed energy source, q is electron charge and V_{oc} is open-circuit voltage.**

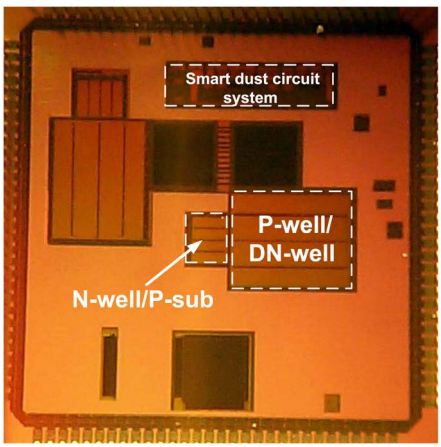

FIGURE 6. **Second chip with resized photodiodes fabricated using UMC 0.25μm CMOS process. N-well/P-sub is 0.2mm^2 and P-well/DN-well is 1.3mm^2.**

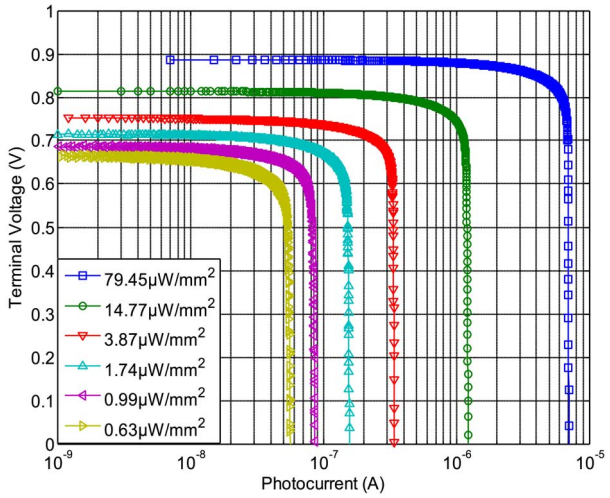

FIGURE 7. **Measured load lines of the resized photodiodes in the second chip under a few different illumination intensities.**

TABLE 1. **Available voltages and currents at the max. power points.**

Illumination intensity (μW/mm^2)	79.45	14.77	3.87	1.74	0.99	0.63
Voltage (V)	0.8	0.7	0.65	0.6	0.55	0.5
Current (nA)	6240	1140	315	145	81	53

The resized photodiodes are measured with a few different illumination intensities and the load lines are shown in Fig. 7. Eye safety restrictions mean that , the maximum illumination intensity from a 830nm laser is 79.45μW/mm^2. The generated voltages and available currents of the photodiodes at the maximum power points are summarized in Table 1. The optically powered energy source can supply a voltage from 0.5V to 0.8V and a current from nano-amperes to micro-amperes at its maximum power point. The efficiency of the energy source is approximately 3.5% when illuminated by light with a wavelength of 830nm.

In order to power the circuit on the same chip using the photodiodes, connections of the energy source are shown in Fig. 8. All the CMOS circuits should sit in a DN-well connected to the P-well terminal of P-well/DN-well photodiode to isolate them from the substrate and the circuits should be covered by a metal layer to block the illumination. The ground of the circuit is then connected to the N-well terminal of N-well/P-sub photodiode. A smart dust circuit system was also fabricated on the second chip marked in Fig. 6. The proposed energy source can successfully power the smart dust requiring the voltage input in the range of 0.5V to 0.85V under illuminations. This smart dust system contains a photodetector, data recovery circuit, instruction decoding circuit and passive optical transmitter driving circuit and this system works as a communication platform for the optical wireless sensor networks [8].

IV. CONCLUSION

The traditional energy source component occupies a significant fraction of the volume of smart dust nodes. This paper introduced an optically powered energy source which can be integrated on the same IC chip as the smart dust circuits. Based on the standard UMC CMOS process, all the possible combinations of two P-N junctions in series were analyzed.

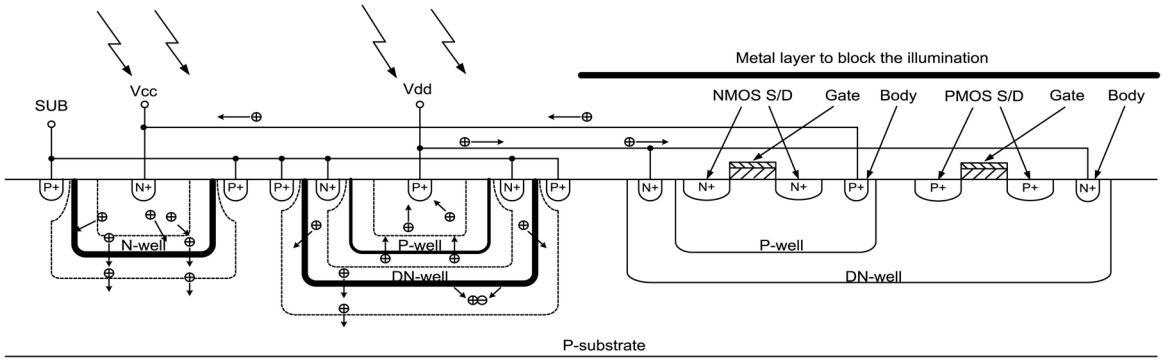

FIGURE 8. **Connections of the proposed energy source to CMOS circuits.**

From the measurement results, only the P-well/DN-well and N-well/P-sub connected in series can generate a voltage different from 0.5V to 0.8V, which is capable of driving circuits. Although the conversion efficiency is approximately 3.5% at 830nm, enough power was available to power an example nano-power sensor node. In many circumstances additional power can be obtained from ambient light.

REFERENCES

[1] C. Y. Chong and S. P. Kumar, "Sensor network: Evolution, opportunities, and challenges," *Proc. IEEE*, vol. 91, no. 8, pp. 1247–1256, Aug. 2003.

[2] T. Nagayama, T. Hirose, Y. Osaki, N. Kuroki, and M. Numa, "A 105-nW CMOS thermal sensor for power-aware applications," in *Proc. IEEE Sensors*, Limerick, Ireland, Oct. 2011, pp. 1265–1268.

[3] T. Shimamura *et al.*, "Nano-watt power management and vibration sensing on a dust-size batteryless sensor node for ambient intelligence applications," in *Proc. IEEE Int. Solid-State Circuits Conf. Dig. Tech. Papers (ISSCC)*, San Francisco, CA, USA, Feb. 2010, pp. 504–505.

[4] S. J. Marinkovic and E. M. Popovici, "Nano-power wireless wake-up receiver with serial peripheral interface," *IEEE J. Sel. Areas Commun.*, vol. 29, no. 8, pp. 1641–1647, Sep. 2011.

[5] J. M. Kahn and K. S. J. Pister, "Next century challenges: Mobile networking for 'Smart Dust'," in *Proc. 5th Annu. ACM/IEEE Int. Conf. Mobile Comput. Netw.*, Seattle, WA, USA, 1999, pp. 271–278.

[6] B. Warneke, B. Liebowitz, and K. S. J. Pister, "Smart dust: Communicating with a cubic-millimeter computer," *Computer*, vol. 34, no. 1, pp. 44–51, Jan. 2001.

[7] J. J. Liu, Y. M. Zhou, G. F. Faulkner, D. C. O'Brien, and S. Collins, "Optical receiver front end for optically powered smart dust," *Inte. J. Circuit Theory Appl.*, to be published.

[8] D. C. O'Brien, J. J. Liu, and G. E. Faulkner, "Design and implementation of optical wireless communications with optically powered smart dust motes," *IEEE J. Sel. Areas Commun.*, vol. 27, no. 9, pp. 1646–1653, Dec. 2009.

[9] H. J. Yoon, S. Itoh, and K. Shoji, "A CMOS image sensor with in-pixel two-stage charge transfer for fluorescence lifetime imaging," *IEEE Trans. Electron Devices*, vol. 56, no. 2, pp. 214–221, Feb. 2009.

[10] S. Kim, J. Kim, B. Kang, and K. Lee, "A CMOS image sensor based on unified pixel architecture with time-division multiplexing scheme for color and depth imaging acquisition," *IEEE J. Solid-State Circuits*, vol. 47, no. 11, pp. 2834–2845, Nov. 2012.

[11] J. P. Crooks *et al.*, "A CMOS image sensor with in-pixel ADC, timestamp and sparse readout," *IEEE Sensors J.*, vol. 9, no. 1, pp. 20–28, Jan. 2009.

[12] B. Choubey, "A wide dynamic range CMOS pixel with Steven's power law response," *Proc. SPIE*, vol. 7780, Aug. 2010, Art. ID 778015.

[13] K. N. Glaros and E. M. Drakakis, "Self-biased logarithmic photoreceptor with low settling time," *IEEE Trans. Circuits Syst. I, Reg. Papers*, vol. 59, no. 10, pp. 2244–2251, Oct. 2012.

[14] D. Das and S. Collins, "A circuit that creates a logarithmic response from an integrating CMOS pixel," in *Proc. 2011 IEEE IEEE Int. Symp. Circuits Syst. (ISCAS)*, pp. 2201–2204.

[15] K. Iiyama, H. Takamatsu, and T. Maruyama, "Hole-injection-type and electron-injection-type silicon avalanche photodiodes fabricated by standard 0.18um CMOS process," *IEEE Photon. Technol. Lett.*, vol. 22, no. 12, pp. 932–934, Jun. 15, 2010.

[16] W. K. Huang, Y. C. Liu, and Y. M. Hsin, "A high-speed and high-responsivity photodiode in standard CMOS technology," *IEEE Photon. Technol. Lett.*, vol. 19, no. 4, pp. 197–199, Feb. 15, 2007.

[17] M. K. Law and A. Bermak, "High-voltage generation with stacked photodiodes in standard CMOS process," *IEEE Electron Device Lett.*, vol. 31, no. 12, pp. 1425–1427, Dec. 2010.

[18] C. Shi *et al.*, "Characterization and optimization of the stacked-PN junction photodiodes structure for energy harvesting CMOS image sensor," in *Proc. 5th Int. Symp. Photoelectron. Detect. Imaging (ISPDI)*, vol. 8908, 2013.

[19] L. Castäaner and S. Silvestre, *Modelling Photovoltaic Systems Using PSpice*. Chichester, U.K.: Wiley, 2002, pp. 20–21.

JING JING LIU received the B.Eng. (1st class Hons.) (2003) and M.Eng. (2005) degrees in electronics engineering from Nanyang Technological University, Singapore, and the D.Phil. degree from the Department of Engineering Science, University of Oxford, Oxford, U.K., in 2009. He worked as an IC Design Engineer with International Rectifier Southeast Asia, Singapore, for half a year in 2005. From 2009 to 2010, he did the Post-Doctoral Research with the University of Oxford. He is currently with Fujian Agriculture and Forestry University, Fuzhou, China, and also a Scientist with the Kuang-Chi Institute of Advanced Technology, Shenzhen, Guangdong, China. His research interests include CMOS subthreshold circuit design and RFIC design.

GRAHAME FAULKNER was born in Oxford, U.K., in 1962. He received the B.Sc. (Hons.) degree in physics and microelectronics from Oxford Brookes University, Oxford, in 1992. He joined the Department of Engineering Science, University of Oxford, Oxford, in 1986 and is currently a Teaching and Research Assistant. His research interests include free space optical communications.

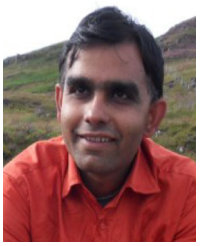

BHASKAR CHOUBEY (SM'11) is an Associate Professor of Engineering Science with the University of Oxford, Oxford, U.K. He received the B.Tech. degree from Regional Engineering College, (now National Institute of Technology), Warangal, India, with a Gold Medal for Best Outgoing Student and the doctorate degree from the University of Oxford as a Rhodes Scholar. Prior to joining Oxford in 2013, he was a Lecturer of Electronics Design with the University of Glasgow, Glasgow, U.K. In past, he has been associated with the Max Planck Institute of Brain Research, Frankfurt, Germany, University of Sydney, Sydney, NSW, Australia, and North West University, Potchefstroom, South Africa. His research interests include CMOS image sensor, nonlinear dynamics, human visual system, and microelectromechanical systems. He has been awarded with the IEEE Sensor's Council GOLD Early Career Achievement Award for his research in sensors and the Myril B. Reed Best Paper Award from IEEE Midwest symposium of circuits and systems.

JIA LIU received the B.Sc. (2009) and M.Sc. (2012) degrees from the Department of Computer Science and Technology, Wuhan University of Technology, Wuhan, China. From 2010 to 2011, she was a Visiting Student working with EDA Lab at the Department of Computer Science, Tsinghua University, Beijing, China. In 2012, She was an intern in one of the core departments with FC-star team members in Baidu Co., Ltd., Beijing, China. She is currently a Product Design Manager with National Supercomputing Center, Shenzhen, China. Her research interests include 3D IC design and physical optimization.

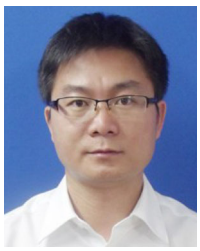

RI QING CHEN received the M.Sc. degree in communications and signal processing with Distinctions from Imperial College London, London, U.K., in 2004 and the D.Phil. degree in engineering science from the University of Oxford, Oxford, U.K., in 2010. He is currently lecturing at the College of Computer Science and Information Technology, Fujian Agriculture and Forestry University (FAFU), Fujian, China. His research interests include wireless communications, spread sequence, signal processing, and wireless sensor technologies.

DOMINIC C. O'BRIEN, photograph and biography not available at the time of publication.

STEVE COLLINS, photograph and biography not available at the time of publication.